

Remote Sensing of Snow in the Solar Spectrum: Experiments in the French Alps

M. Fily

Laboratoire de Glaciologie et Géophysique de l'Environnement, CNRS/UJF, Grenoble, France

and

J.P. Dedieu

Laboratoire de la Montagne Alpine, CNRS/UJF, Grenoble, France

and

Y. Durand and C. Sergent

Centre d'Etudes de la Neige, Météo-France, Grenoble, France

ABSTRACT

Two experiments were performed in April and December 1992 in the French Alps using simultaneous remote sensing and ground truth data. Snow grain size and soot content of samples collected in the field were measured. The Landsat thematic mapper (TM) sensor was used because it has a good spatial resolution, a middle infrared channel which is sensitive to grain size and a thermal infrared channel. First, the reflectance data were compared with the theoretical results obtained from a bidirectional reflectance model. Then, some remote sensing-derived snow parameters were compared with the output of a snow metamorphism model (CROCUS), viz., lower elevation of the snowcover, the surface grain size and the surface temperature. A digital elevation model was used to obtain the local incidence angles and the elevation of each snow pixel. The pixels were then grouped according to CROCUS classification (range, elevation, slope, and orientation) and the mean snow characteristics for each class were compared with the CROCUS results. The lower limit of snow and the surface grain size derived from TM data were compared favourably with the model results. Larger differences were found for the temperature, because it varies rapidly and is very sensitive to shadowing by the surrounding mountains and also because its remote measurement is dependent on atmospheric conditions.

INTRODUCTION

For climatological studies^{1,2}, avalanche forecasting^{3,4}, and water resource management, it is necessary to measure and compute the main snow characteristics: area, depth, water equivalent, albedo, snow type, etc. Snow-covered areas are often not easily accessible; remote sensing is, therefore, an adequate tool for their study on them. To reach these goals, many experiments were carried out at

different locations in the French Alps with simultaneous remote sensing and ground truth data^{5,6}. Those experiments were restricted to the solar spectrum spectral range. In the visible part of the solar spectrum, snow reflectance depends mainly on the concentration of pollutants. The near-infrared reflectance is dependent on the snow grain geometry, that is, shape and size⁷. Other characteristics are of interest in the microwave range.

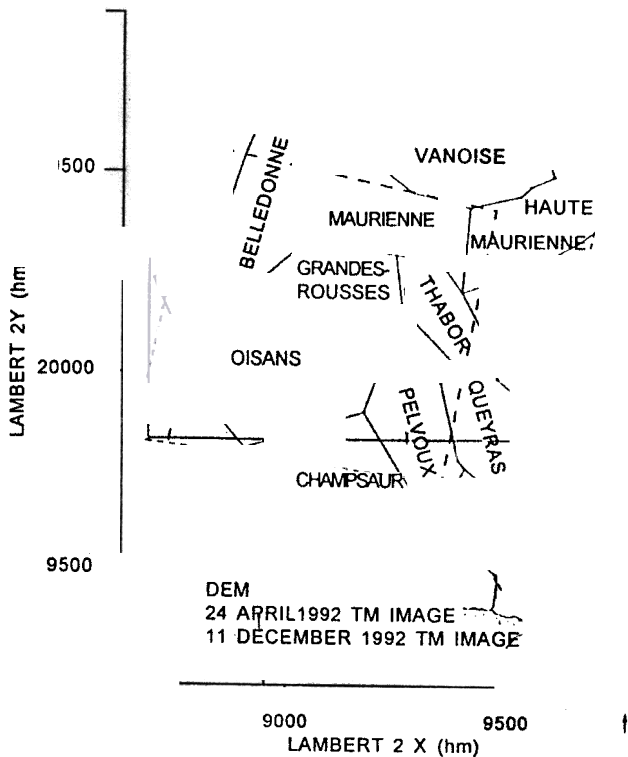


Figure 1. Geographical location of the ranges studied with the limits of the Landsat images and of the available digital elevation model.

In this paper, the authors have reported about ground data and remotely-sensed data and their processing. Model results (snow reflectance model and CROCUS) and measured results have been compared. The parameters compared are the lower limit of the snowcover elevation, its temperature and surface grain size.

2 GROUND DATA

The study area is located in a highly mountainous terrain in the French Alps (Fig. 1). Eleven sites were selected for ground measurements; they are spread over a large range of elevations (1850-3320 m) and slope directions; so several different types of snow were found.

Each site was located precisely on a map and the main features of the topography (slope angle and direction) were recorded. At the time of remote sensing data acquisition, temperature, snow density and its liquid water content (when necessary) were measured at each site. A careful stratigraphy of the upper 30 cm of snow was conducted, where the type and size of grains were evaluated *in situ*.

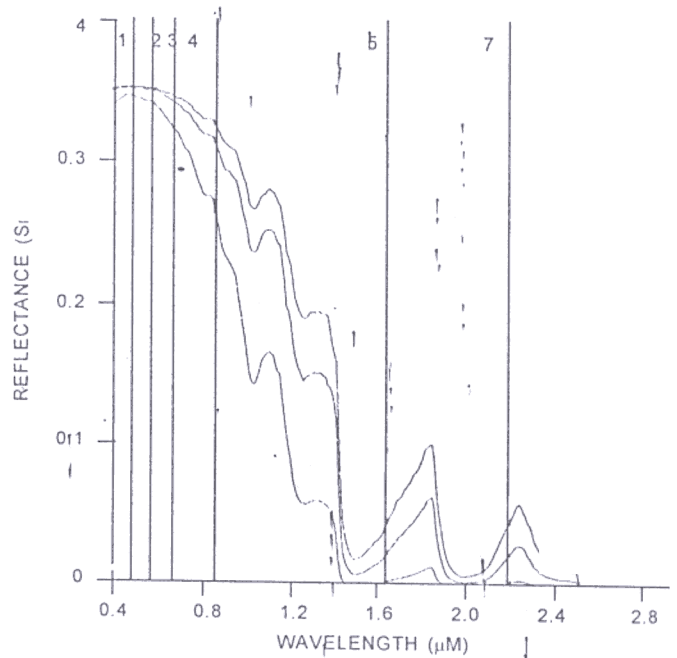


Figure 2. Modelled bidirectional reflectances for three different grain sizes (50 μm , 100 μm and 500 μm) vs the wavelength. The incident sun angle is 40° for a nadir view. Vertical lines denote the Landsat TM channels.

Moreover, snow samples were collected in the field and maintained in iso-octane below 0°C to prevent metamorphism⁸ and were analysed in a cold room at Grenoble. For each snow sample, video macrophotographic pictures were made and digitised. Using an image analysis system, the mean convex radius of curvature of randomly chosen clusters of 30-50 different crystals was computed. The mean convex radius of snow grains can be taken as an objective snow grain size indicator. In an earlier study⁹, a relationship was established between this parameter and the theoretical spherical radius according to Wiscombe and Warren modelling¹⁰. Therefore, the mean convex radius was taken as the ground reference measurement of grain size.

3 REMOTE SENSING DATA

Two Landsat 5 thematic mapper (TM) images, quarter scenes, were acquired, on 24 April and 11 December 1992 at 9:45 U.T. (Fig. 1). The solar incidence angle was 39.9° in April and 69.1° in December 1992. The main spectral characteristics of TM channels are given in Table 1. The spatial resolution is 30 m for channels 1, 2, 3, 4, 5, 7 and

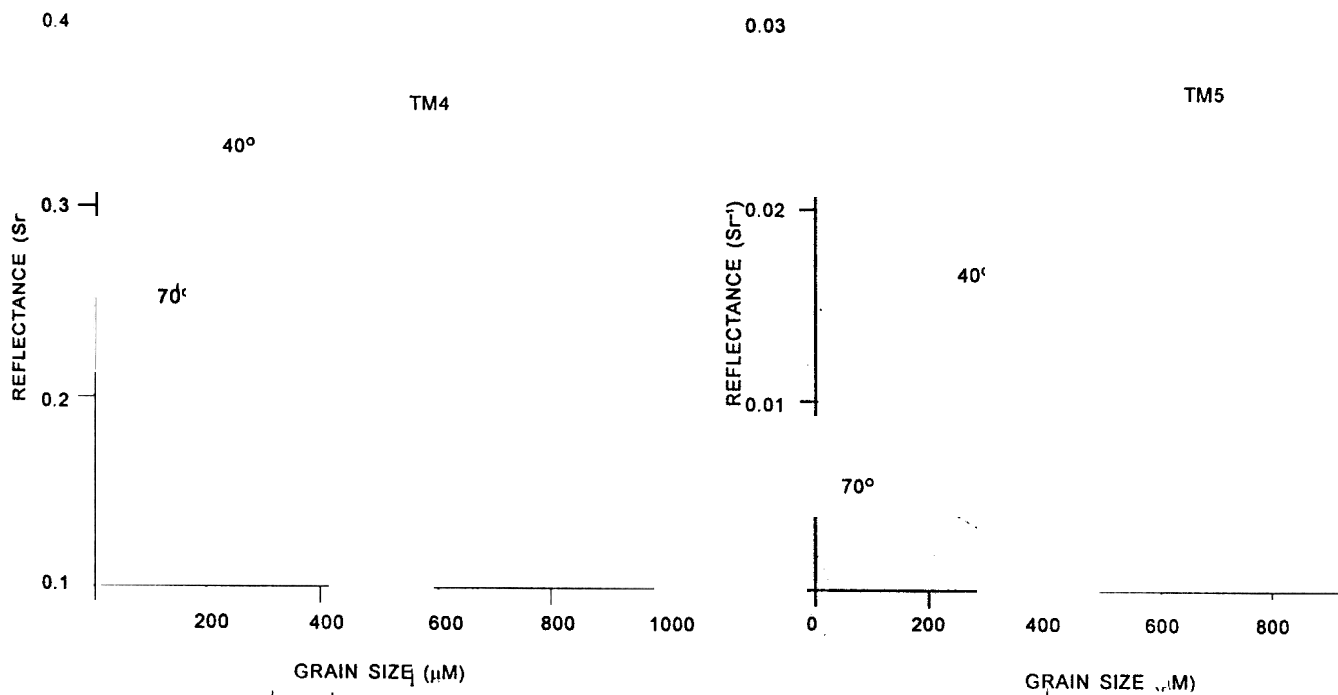


Figure 3. Modelled reflectances vs grain size for two different wavelengths: 0.85 μm [TM4, Fig. 3(a)] and 1.65 μm [TM5, Fig. 3(b)]. The surface is horizontal, the sun incidence angle is 40° (April) or 70° (December) and the view is nadir.

120 m for channel 6. On 24 April 1992, the sky was clear with only a few small clouds. On 11 December 1992, the upper limit of the clouds was at 1200 m corresponding to the lower limit of the snowcover; above, the sky was clear, except for some cirrus (1/8 to 2/8 cover). The images were geolocated using a resampling method with a set of ground control points. The location error on each pixel was estimated to be <100 m.

The snow reflectances were computed from Landsat data for each channel. To get the radiance (L_{sat}) at the satellite level from numerical counts (CN) given on the tape, the pre-flight calibration

Table 1 Spectral characteristics of the 7 channels of the Landsat 5 thematic TM mapper sensor

Channel Nos	Spectral characteristics (μm)	
TM1	0.45	0.52
TM2	0.52	0.60
TM3	0.63	0.69
TM4	0.76	0.90
TM5	1.55	1.75
TM6	10.40	12.50
TM7	2.08	2.35

coefficients given with the images were used. Values of solar exo-atmospheric irradiance, E_0 , were reported by Markham and Barker¹¹.

Because the slope of each site is known, the local incidence angle, θ_i , of sun irradiance can be computed and, therefore, the apparent reflectance at the top of the atmosphere, ρ_{app} , is:

$$\rho_{\text{app}} = L_{\text{sat}} / (E_0 * D * \cos \theta_i)$$

where D is a sun-earth distance factor ($D = 0.9890$ in April 1992 and $D = 1.0324$ in December 1992).

An atmospheric correction was applied to get the ground reflectance, ρ_{gr} , using the 6S atmospheric transfer model, which is an improved version of the 5S atmospheric transfer model described by Tanré¹², *et al.* All the reflectances used hereafter are given with ρ_{gr} and without ρ_{app} atmospheric correction to determine if this correction is important.

4. SNOW REFLECTANCE MODEL

The bidirectional reflectance of snow is computed with a model based on the resolution of the radiative transfer equation by discrete ordinate method¹³. The snow is assumed pollution-free, because one

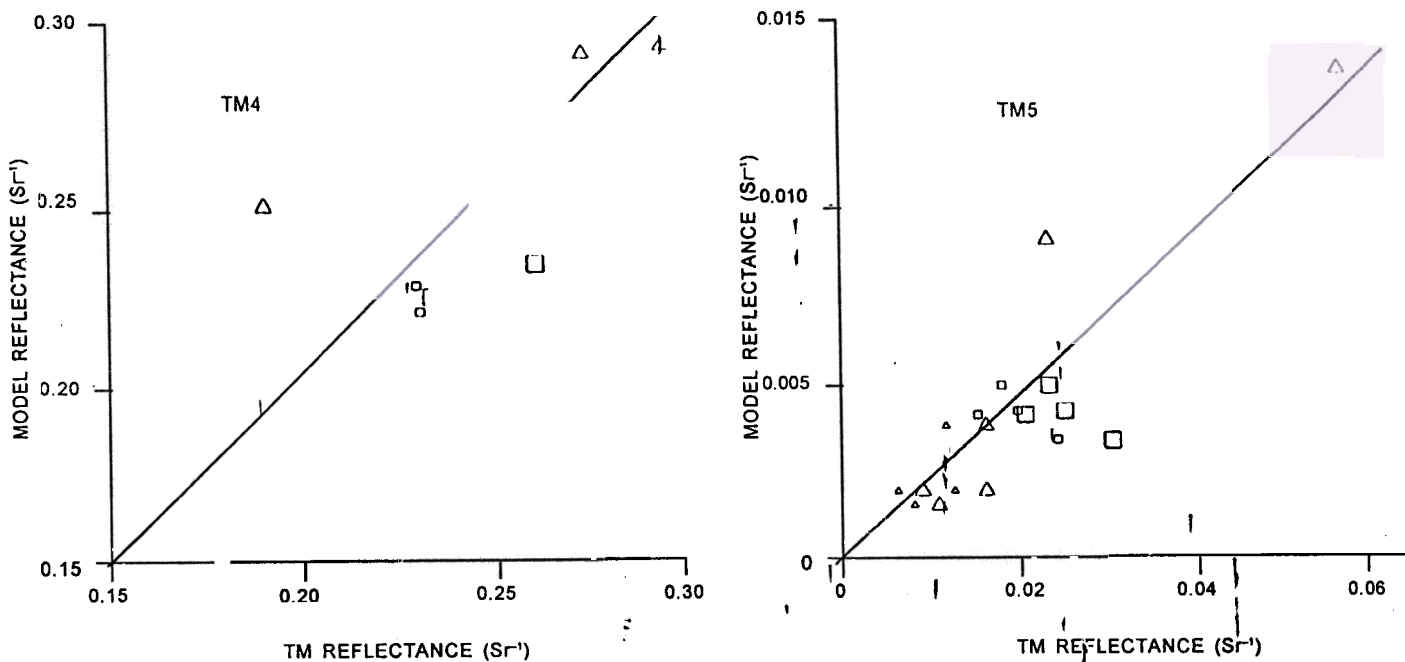


Figure 4. Modelled bidirectional reflectances vs measured reflectances derived from channels TM4(a) and TM5(b). The model results were obtained using ground data for grain size and the real geometrical conditions. Triangles are for April, squares for December, small symbols are without atmospheric corrections, large symbols with atmospheric corrections.

is mostly interested in the near-infrared channels which are independent of pollution level⁷. Also, because the penetration depth is small in the near-infrared, a single layer of snow with a single grain size was always considered.

A plot of bidirectional reflectance, ρ_b , obtained from the model against the wavelength for three grain sizes (50 μm , 100 μm and 500 μm) is shown in Fig. 2. The bidirectional reflectance is in Sr^{-1} ; the reflectance of a lambertian surface would be obtained by multiplying ρ_b by π . The use of ρ_b was preferred because the snow is not lambertian, the slopes are important in alpine areas and measurements are made in a single direction.

Another way to show the dependence of reflectance on the grain size is depicted in Fig. 3. In this figure, the bidirectional reflectance is computed for a horizontal surface at a nadir view for two solar incidence angles (40° for April and 70° for December 1992) and for two channels (TM4 and TM5). The results for TM7 are almost the same as for TM5. From these curves, it is clear that the grain size can be obtained theoretically from the reflectance, but also that a precise value of the reflectance is

needed to do so. For TM4, the curves are flat and highly dependent on the incidence angle; a small error in reflectance induces a large error in grain size. For TM5 and TM7, there is a saturation effect for large grains. It is, therefore, difficult to measure those large grains precisely.

The modelled bidirectional reflectances for channels TM4 and TM5 against the Landsat-derived bidirectional reflectances are given in Fig. 4. The modelled reflectances are obtained using the surface-measured mean convex radius and the real slope. Each Landsat-derived reflectance is given, with and without atmospheric corrections. The effect of atmospheric correction on the reflectance is important for TM4, but not for TM5.

For TM4, most of the April data are close to the theory, except for site No. 6. This site was surrounded by forest with a lower reflectance than the snow and the environment effects were overestimated. Although the snowcover was homogeneous, December-corrected reflectances were too large and scattered. It is mainly due to the topography. In the case of a low sun elevation, as in December, the irradiance coming from the

facing slopes cannot be neglected, as was shown by Proy¹⁴, *et al.* This effect is important for TM4, because the snow reflectance is high. In contrast, the reflectance of TM5 is very low, so that this effect becomes negligible. The variation of reflectance against grain size is small at 0.85 μm compared to other factors: Sun incidence angle and atmosphere. The Landsat-derived reflectance for TM4 is not accurate enough to allow an inversion of the grain size from the reflectance.

For TM5 and TM7, the Landsat-derived reflectances are 4 or 5 times larger than the model results. The main reason for the discrepancy seems to be that the optical size of the grains is much smaller than the measured mean convex radius. The penetration depth at this wavelength is so small that the shape of the grains is very important. More measurements of BRDF are clearly needed in this spectral range with simultaneous grain size measurements. Nevertheless, the variations of reflectances due to grain size, slope and solar incidence angle are well reproduced for TM5, as shown by the linear fit between modelled and Landsat-derived reflectances (Fig 4). It is then possible to try to deduce the grain size from the reflectance if an empirical correction is done (for TM5: $\rho_{corr} = 0.4 * \rho_{gr}$). Then the radius corresponding to the corrected reflectance and the geometric conditions of irradiance, measurement and slope are searched by an iterative process using the model of Stamnes¹³, *et al.* The results are given in Fig. 5. There is a good overall agreement between ground measurements and Landsat-derived data, because the authors used an empirical correction fitted on the same data. An interesting result is that the same correction is used for all the data and, therefore, it is possible to extrapolate this scheme to the whole image.

The same inversion procedure was used with the Landsat-derived reflectance instead of the corrected reflectance. The computed radii are smaller than the measured mean convex radii, but there is still a linear relationship between the measurements and the model results. The main problem is that the computed radii are different for TM5 and TM7 and that those small sizes would not fit with the TM4 data. Therefore, optical grain size is different for different wavelengths. This effect was confirmed

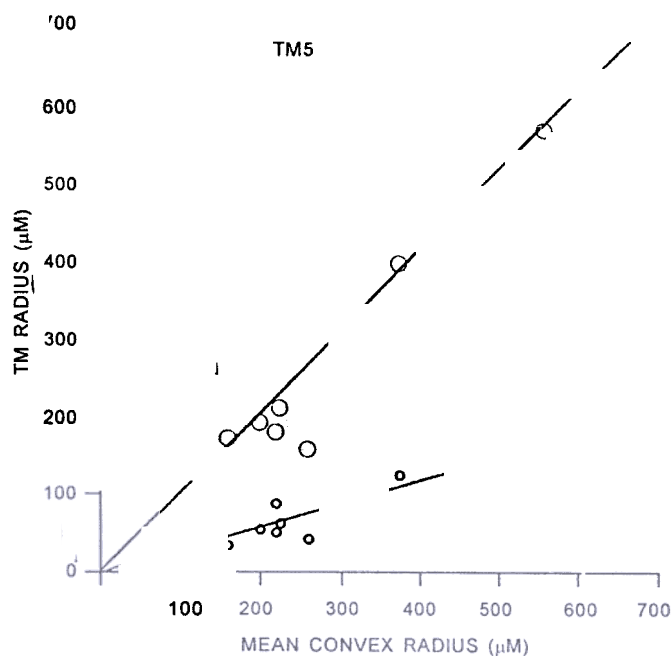


Figure 5. Comparison between the measured snow grain mean convex radius and the grain size derived from Landsat TM5 data after an empirical correction of the reflectance (large circle), and without the correction (small circle).

by new laboratory measurements made at the Centre d'Etude de la Neige at Grenoble, but more studies are needed to better determine the size parameters that the model must take into account.

5 SNOW METAMORPHISM MODEL & REMOTE SENSING-DERIVED SNOW PARAMETERS

5.1 CROCUS Snow Metamorphism Model

Snowcover evolution at a given location depends mainly on the prevailing meteorological conditions. They govern its energy and mass balance and, therefore, the metamorphism of each layer. They also govern the presence of liquid water inside the snowcover. A physically-based numerical model, called CROCUS, has been developed to simulate all these phenomenas^{3,4}. It derives a complete description of the snowcover, including temperature, density, liquid water content, age and stratigraphy of the different layers as a function of the prevailing meteorological conditions.

In many applications, a complete series of meteorological observations are not available at particular experiment points. For these reasons, a

meteorological objective analysis model, called SAFRAN, was developed¹⁵ to provide CROCUS with its necessary input data. It is aimed to establish hourly surface meteorological conditions at different idealised particular points of the alpine ranges. Based on statistical interpolation, it uses all the available observations as well as numerical meteorological forecasts. It provides an hourly diagnosis of air temperature, wind, humidity, cloudiness, rainfall, snowfall and surface radiations.

Using SAFRAN + CROCUS, the snow mantle characteristics are computed every hour for many ranges in the French Alps (Fig. 1), at all elevations by steps of 300 m, for three ground slopes (horizontal, 20°, 40°) and six orientations (N, E, SE, S, SW, W). This model has been in use for operational snow avalanche forecasting in France since 1992. It is operated by the French Weather Forecasting Service Météo-France.

Two CROCUS characteristics are of importance for this study:

Shadowing by the surrounding mountains is not considered.

There is no re-initialisation of the snow mantle characteristics during winter.

The CROCUS model begins to operate in August at the first snowfall and runs independently until the following July using only new meteorological input from SAFRAN. It means that eventual errors, on snow depth for example, can propagate over a long period.

5.2 Remote Sensing Data Processing

A digital elevation model (DEM) was used to obtain the elevation, slope and azimuth of each pixel or group of pixels. The grid size of DEM is 250 m. It was considered that this resolution was good enough considering the inaccuracy of the pixel location, because the TM6 spatial resolution is only 120 m and, more generally, because it is difficult to obtain precise DEM in alpine areas.

For temperature and grain size studies, pixels are grouped in cells of 8 × 8 pixels which correspond to 2 × 2 TM6 pixels. Therefore, the size of a cell

is 240 × 240 m, close to DEM resolution. A visible channel (TM2) is used to select snow from other ground surfaces (bare soil, water, vegetation) and a ratio between TM5 and TM4 is used to distinguish clouds.

For the lower limit of snow mantle, single pixels were used instead of groups to obtain the exact number of snow pixels for area determination and because the absolute radiance was not used. The elevation, slope and azimuth of each pixel were then interpolated from DEM. The computed slope and azimuth are, therefore, representative of an area larger than one pixel.

In order to compare Landsat-derived parameters with the CROCUS output, pixels or cells must be grouped into different classes which are equivalent to the CROCUS classes. There are six azimuth and three slope classes (Table 2). Further processing of the TM data is slightly different for each parameter.

5.3 Lower Limit of Snowcover

The lower limit of the snowcover is different for each range, because the meteorological conditions are different. Slope and azimuth are also influential. On north-oriented slopes, the snow should be present on the ground at a lower elevation than on south-oriented slopes, because there is less solar irradiance. Comparisons were made between CROCUS and TM-derived lower elevations for 24 April 1992 images. This date was chosen because the lower elevation range is larger at the end of winter and because the upper limit of the clouds was too close

Table 2. Different azimuths and slopes used in the CROCUS model (discrete values) and the corresponding chosen Landsat classes

CROCUS	Azimuth		Slope		
	Landsat	CROCUS	Landsat	CROCUS	Landsat
North	292.5° to 67.5°	South	17.5° to	Horizontal	0 - 10°
East	67.5° to 112.5°	South-west	202.5° to 247.5°	20°	10°-30°
South-east	112.5° to 157.5°	West	202.5° to 247.5°	40°	>30° or 35°-45°

lower limit of snow in December 1992

CROCUS Model Lower Limit

For each class, by increment of 300 m, CROCUS computes the snow depth. The lower limit is taken as the maximum elevation between the upper CROCUS level where there is no snow, and the zero snow depth level computed from linear extrapolation using the given snow depths at higher elevations.

Landsat TM Lower Limit

The classification of snow pixels was based on TM3 only, because the clouds were at high elevation and did not modify the results. A simple threshold on the numerical count was easily chosen, because the difference between the snow and the other surfaces was clear for the sunny pixels^{16,17}. Shaded snow pixels were not selected, though there were a few of them, because the sun incidence angle was only 39.9°. For each class (range, elevation, azimuth, and slope), the total number of pixels and the number of selected snow pixels were counted. The elevation increment was 100 m, smaller than the CROCUS increment. Two lower limits were then defined as the elevations where 30 per cent or 50 per cent of the surface was snow covered. The 30 per cent threshold was chosen to take into account the possible effect of shadowed pixels.

5.3.3 *CROCUS & Landsat Lower Limits*

The results are given in Fig. 6. Globally, it appears that for CROCUS and Landsat, the snow limit is lower on north and east-oriented slopes than on south-oriented slopes, that the differences between different azimuths are larger when the slope is 40°, and that the snow limit is higher for the southern ranges (Pelvoux, Thabor, and Queyras). The overall comparison is good in as much as the model has never been re-initialised since last August.

For the north and west azimuths, some care must be taken with the Landsat-derived estimation because the shadowed pixels were not taken into account, although the 30 per cent limit should minimise this problem. For most cases, the differences between azimuth at 40° slope are more pronounced for CROCUS than those observed from TM data. It

seems in particular that CROCUS overestimated the lower snow elevation for south and south-east slopes in many ranges: Oisans, Pelvoux, Thabor, and Queyras. There were less meteorological data close to the Italian border and the snow accumulation could have been underestimated.

In conclusion, it seems possible to define a lower limit of snow-covered terrain from Landsat data, which is comparable to the CROCUS model output. This is important because no routine observation of the lower limit of snow is available.

5.4 Surface Snow Grain Size

Snow grain size has an important effect on the snow albedo and is, therefore, an important parameter for any study which needs surface radiative balance^{11,18}. But snow grain size is a parameter which is not easy to define: The sizes which are computed by the model, those which are measured *in situ*, and those which are deduced from the reflectance are not the same, although they are certainly related. This difficulty must not be forgotten when comparing the results. Because the depth of penetration of near-infrared and middle-infrared electromagnetic waves in the snow is very small^{7,19}, only the surface grain sizes were studied.

5.4.1 *CROCUS Model Grain Size*

As seen above, snow grain size is one of the physical characteristics which is computed by the CROCUS model for avalanche forecasting. It is defined in terms of both optical size for albedo computation and physical size for stability assessment.

5.4.2 *Landsat TM Grain Size*

The same inversion technique as described above was used to determine the grain size. The atmospheric correction was applied on the mean radiance of each group of 8 × 8 pixels before the reflectances were averaged within different classes. To show the effects of atmospheric correction, the example of the April TM4 data for the Oisans range was chosen in the extreme case of steep slopes (40° slope class) for which the local incidence is highly dependent on azimuth (Fig. 7). There is a factor 2 between the radiances of the west-oriented surfaces

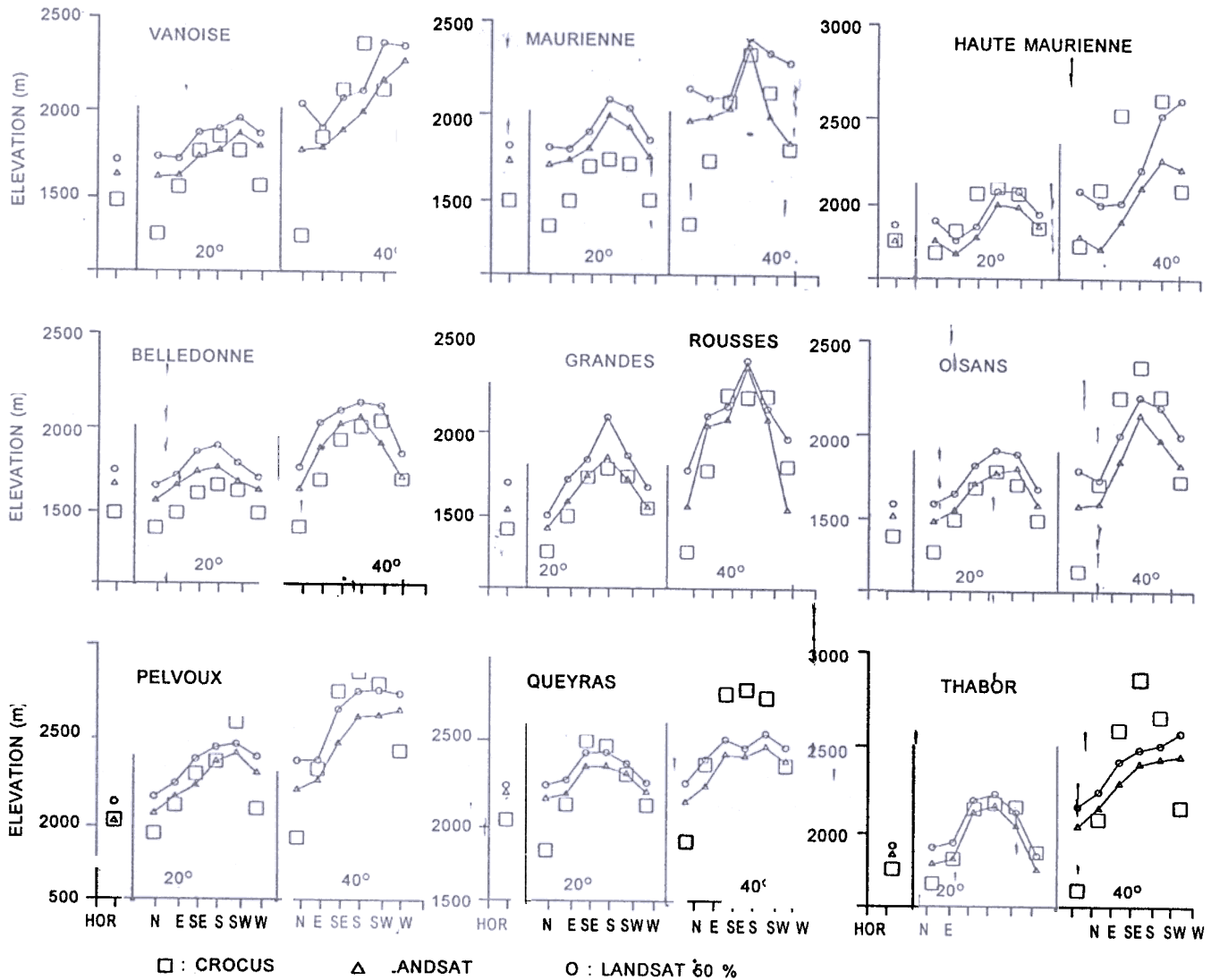


Figure 6. Lower elevation of the snowcover on 21 April 1992, for the ranges studied according to the slope (horizontal, 20°, 40°) and to the orientation (N,E,SE,S,SW,W). Two different thresholds of the percentage of snow-covered pixels are used to define the lower limit from Landsat data (30 per cent and 50 per cent).

and those of the south-east-oriented surfaces. The final surface reflectances, after atmospheric correction, are almost independent of the azimuth.

5.4.3 CROCUS & Landsat TM-Derived Snow Grain Sizes

The April 1992 image was used for this study, because the snow surface grain sizes varied widely, while they were uniform in December 1992. The inversion technique was first applied to TM5 and TM7 channels. The results were identical for both channels and, therefore, only the TM5 results are described. The inversion was applied to all the

ranges, but only for horizontal surfaces because the results for tilted surfaces vary only slightly. The grain sizes obtained from the two very different techniques compared nicely (Fig. 8). There is an altitudinal variation for both CROCUS and TM5 results, the smallest grains being at high elevation.

The inversion technique was also applied to the TM4 data. Unfortunately, the results were rather disappointing, because the variation of grain size with elevation was found to be too large even if the mean value was correct without any tuning. The derived grain sizes are given only for horizontal

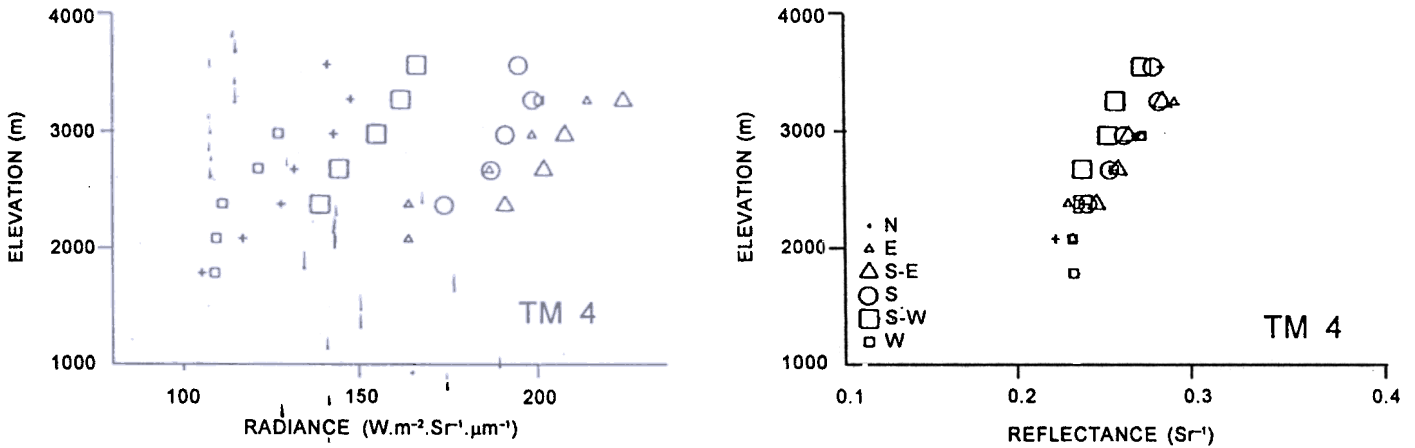


Figure 7. Measured radiances and derived surface snow reflectances after atmospheric corrections for different elevations and orientations, for steep slopes (>30°) in the Oisans range, on 24 April 1992.

surfaces in the Oisans range in Fig. 8. This result is in complete agreement with those of the previous study⁶. The effect of grain size on TM4 reflectance compared to other factors (incidence angle, atmosphere, and indirect irradiance from facing slopes) is so small that any accurate inversion is impossible in

Alpine terrains

To avoid the local incidence angle computations and atmospheric corrections, the authors also tried to use the simple ratio R45 with:

$$R45 = (r5 - r4) / (r5 + r4), r4 \text{ and } r5 \text{ being the}$$

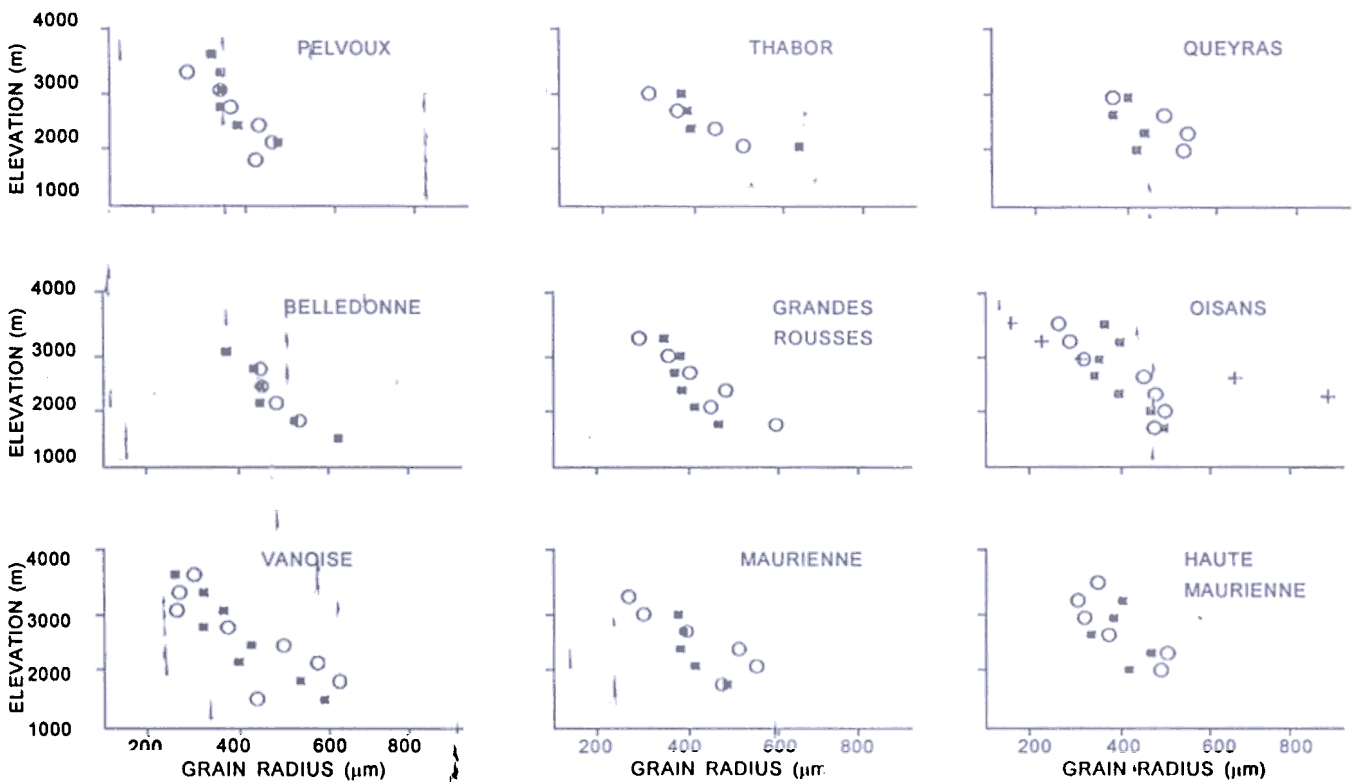


Figure 8. Snow grain sizes modelled by CROCUS (black squares) and deduced from Landsat TM5 data (open circles) for different ranges and elevations, on horizontal surfaces, on 24 April 1992. Grain sizes deduced from Landsat TM4 data (+) are given for Oisans range only.

simple exo-atmospheric reflectances for TM5 and TM4, respectively.

The behaviour of this ratio matched the earlier results and theoretical computations well⁶: It was smaller for smaller grains at high elevation. Yet, it was found to be impossible to invert the ratio to obtain quantitative results, because the slope and the atmospheric effects were not eliminated⁶.

5.5 Surface Snow Temperature

Temperature gradient in the snow mantle is one of the most important factors for snow metamorphism. Determination of a good surface temperature is therefore necessary. Absorption of the thermal infrared electromagnetic wave in the snow is very high^{7,19}. Therefore, only the upper surface of the snow is seen by the thermal infrared channel TM6 (Table 1).

CROCUS Model Temperature

The surface temperature is obtained from the energy balance in the CROCUS model. This balance is very sensitive to the snow albedo (grain size and pollution), to the sensible heat flux and to the atmospheric emission at long wavelengths, which can be extremely variable in Alpine areas.

5.5.2 Landsat TM Temperature

The calibration coefficients to convert digital counts to spectral radiance were reported by Markham and Barker¹¹. Radiance R is then inverted to obtain the snow temperature T_s using the following equation given by Wukelic²⁰, *et al*:

$$T_s = K2 / \ln (K1/R +)$$

where $K1 = 60.776 \text{ mW cm}^{-2} \text{ Sr } \mu\text{m}$ and $K2 = 1260.56 \text{ K}$.

According to Wukelic²⁰, *et al*, the uncorrected TM6 data give good approximations within 1-2 °C of the ground temperature values on clear days. They clearly indicate that using inaccurate atmospheric profiles for a possible atmospheric correction could lead to larger error. Therefore, the authors did not apply any atmospheric corrections, as no local radiosonde was available and because

the sky was clear above 1200 m except for some cirrus in December 1992. Snow emissivity is close to 0.99 in the thermal band^{7,21}. It was assumed that the emissivity was 1, because the induced difference for the temperature would only be 0.5 °C. It was considered that this difference was small compared to other factors, such as atmospheric correction and the sensor calibration.

In conclusion, the temperature uncertainty was estimated to be less than 2 °C where the sky was clear. This value is in accordance with the 0 °C temperature (wet snow) found in April 1992 at a low elevation and with the few *in situ* measurements which were available. This value is nevertheless small compared to the differences between CROCUS and Landsat, as shown here.

5.5.3 CROCUS & Landsat TM Derived Snow Surface Temperature

The results are given only for the Oisans range, 20° slope (April and December 1992) because the differences between ranges are small and the conclusions are the same for other slopes (Fig. 9).

There is less azimuthal variability with TM6, because each class was defined by an azimuth range and not by a discrete value, as for CROCUS. In April 1992, the main reason for discrepancy between the TM6 and the CROCUS results is due to the fact that shadowing by the surrounding mountains was not considered in the CROCUS model which, therefore, overestimated the surface temperatures (0 °C almost everywhere). In December 1992, the remote sensing data tended to underestimate the temperature because they were affected by high thin cirrus clouds (1/8 to 2/8 cover) which are radiatively cold. Unfortunately, the cirrus effect is very difficult to quantify. On the contrary, the CROCUS model tended to overestimate the temperature, because shadowing by the surrounding mountains was not taken into account and the sensible heat flux was based on a very few measurements, especially at high altitudes.

The TM6 temperature is deduced from the energy emitted by a rough surface and modified through the atmosphere when the CROCUS model computes an energy balance for a flat and smooth

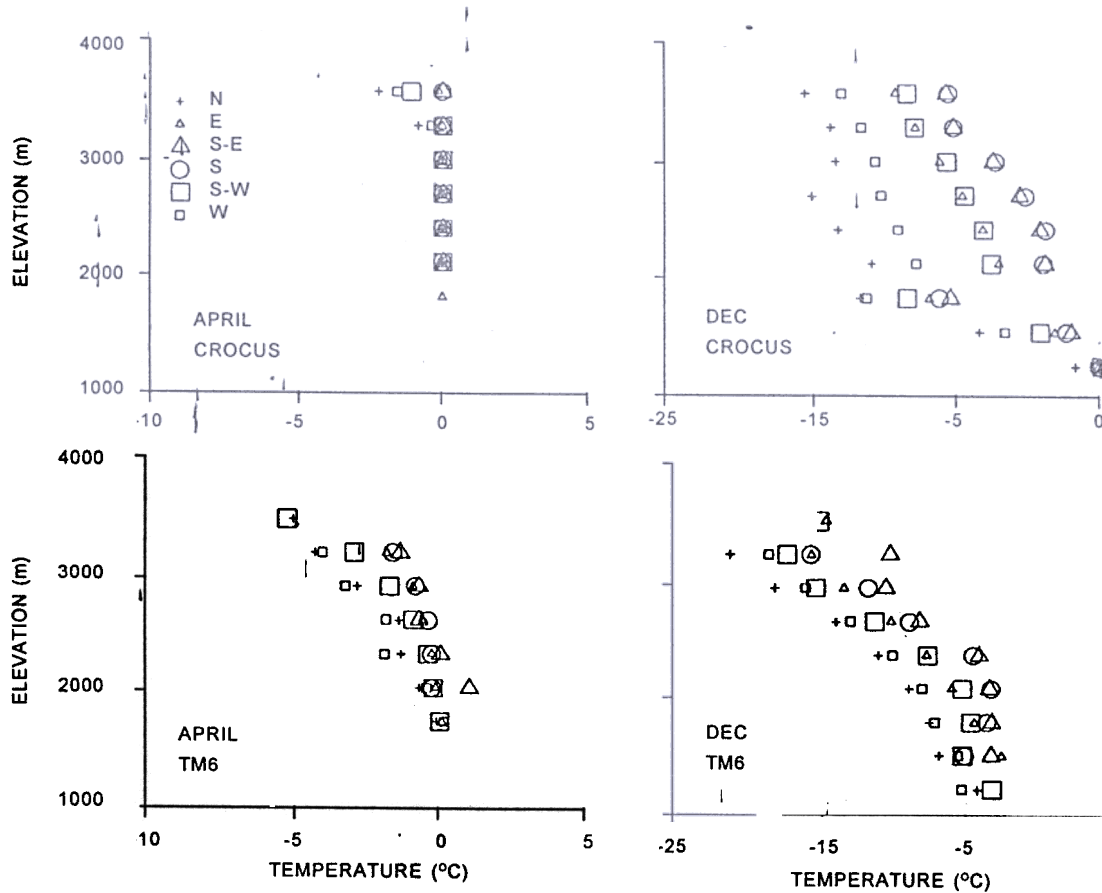


Figure 9. Snow surface temperature for the Oisans range on 24 April and 11 December 1992, modelled by CROCUS (10 U.T.) and deduced from Landsat TM6 data (9:45 U.T.). Results are given for different elevations and orientations at 20° slope.

surface without any shadowing effects by the surrounding mountains. Therefore, care must be taken when comparing these two determinations of the same parameter. In April 1992, one is pretty confident about the TM6 temperature, because the 0 °C found at low elevation is an absolute validation. In December 1992, the 5 °C difference could be attributed partly to CROCUS and partly to the satellite data; only the altitudinal gradient is similar.

6. CONCLUSION

The Landsat TM data associated with a DEM at 250 m resolution can be used to provide some characteristics of the snow mantle in alpine areas which are comparable to the output of a snow metamorphism model (CROCUS). The comparisons can be made for different snow classes according to their geographical location (range), their elevation, slope and orientation.

The lower limit of the snow mantle was defined as snow-covered pixels between 30 per cent and 50 per cent. This matched the limit set by CROCUS, although the model ran without any re-initialisation during the entire winter.

The surface grain size was obtained from the 1.6 µm TM5 channel. The values, which are similar to a mean convex radius, are close to the CROCUS grain size even if it is difficult to precisely define this parameter. An empirical parameter must be used to fit the modelled reflectance to the observed reflectance, because the real grain shape is more complex than the one used in the model. It is impossible to derive snow grain sizes from TM4 in alpine areas, because this channel is also very sensitive to other effects, such as atmospheric conditions, irradiance from facing slopes and local incidence angles, which are not well known.

The surface temperatures were more difficult to compare even though they should be the easiest parameter to define. It was found, for example, that the cirrus were difficult to detect, but were very important when considering the radiative transfer.

ACKNOWLEDGEMENTS

These experiments were funded by the French Programme National de Teledetection Spatiale and the Centre National d'Etudes Spatiales (SPOT4/MIR).

REFERENCES

- Hall, D.K. Assessment of polar climate change using satellite technology. *Review of Geophysics*, 1988, 26(1), 26-39.
- Marshall, S. & Oglesby, R.J. An improved snow hydrology for GCM's, Part 1: Snowcover fraction, albedo, grain size and age. *Climate Dynamics*, 1994, 10, 21-37.
- Brun, E.; Martin, E.; Simon, V.; Gendre, C. & Coleou, C., An energy and mass model of snowcover suitable for operational avalanche forecasting. *Journal of Glaciology*, 1989, 35(121), 333-42.
- 4 Brun, E.; David, P.; Sudul, M. & Brugnot, G. A numerical model to simulate snowcover stratigraphy for operational avalanche forecasting. *Journal of Glaciology*, 1992, 38(128), 13-22.
- Fily, M.; Bourdelles, B.; Dedieu, J.P. & Sergent, C. Comparison of in situ and Landsat thematic mapper-derived snow grain characteristics in the Alps. *Remote Sens. Environ.*, 1997, 59, 452-60.
- 6 Fily, M.; Dedieu, J.P. & Durand, Y., Comparison between the results of a snow metamorphism model and remote sensing derived snow parameters in the Alps. *Remote Sens. Environ.*, 1999, 68, 254-63.
- Warren, S.G. Optical properties of snow. *Rev. Geophys. Space Phys.*, 1982, 20(1), 67-89
- 8 Brun & Pahaut An efficient method for a delayed and accurate characterisation of snow grains from natural snowpacks. *Journal of Glaciology*, 1991, 37(127), 420-22.
- 9 Sergent, C.; Pougatch, E.; Sudul, M. & Bourdelles, B. Experimental investigation of optical properties for various types of snow. *Annals of Glaciology*, 1993, 17, 281-87.
- 10 Wiscombe, W.J. & Warren, S.G. A model for the spectral albedo of snow, part I: Pure snow. *J. Atmos. Sci.*, 1980, 37, 2712-733.
- Markham, B. L. & Barker, J.L. Landsat MSS and TM post-calibration dynamic ranges, exoatmospheric reflectances and at satellite temperatures. *Landsat Technical Notes No. 1*, 1986, 1, 3-8.
- 12 Tanré, D.; Deroo, C.; Duhaut, P.; Herman, M.; Morcrette, J.J. Perbos, J.; & Deschamps, P.Y. Simulation of the Satellite Signal in the Solar Spectrum. Laboratoire d'Optique Atmosphérique, 59655 Villeneuve d'Ascq Cedex, France, p. 115.
- Stamnes, K.; Tsay, S.; Wiscombe, W., & Jayaweera, K. Numerically stable algorithm for discrete-ordinate-method radiative transfer in multiple scattering and emitting layered media. *Applied Optics*, 1988, 27, 2502-509.
- 4 Proy, C.; Tanré, D. & Deschamps, P.Y. Evaluation of topographic effects in remotely sensed data. *Remote Sens. Environ.*, 1989, 30, 21-32.
- 5 Durand, Y.; Brun, E.; Merindol, L.; Guyomarch, G.; Lesaffre, B. & Martin, E. A meteorological estimation of relevant parameters for snow models. *Annals of Glaciology*, 1993, 18, 65-71
- 6 Dozier, J. & Marks, D. Snow mapping and classification from Landsat thematic mapper data. *Annals of Glaciology*, 1987, 9, 97-103.
- 7 Dozier, J. Spectral signature of alpine snow cover from the Landsat thematic mapper. *Remote Sens. Environ.*, 1989, 28, 9-22.
- 8 Grenfell, T.C.; Warren, S.G. & Mullen, P.C. Reflection of solar radiation by the Antarctic snow surface at ultraviolet, visible, and near-infrared wavelengths. *J. Geophys. Res.*, 1994,

- 99(D9), 18 669 8-684
19. Warren, S.G. Optical constants of ice from the ultraviolet to the microwave. *Applied Optics*, 1984, 23(8), 1206-225.
 20. Wukeljc, G.E.; Gibbons, D.E.; Martucci, L.M. & Foote, H.P. Radiometric calibration of Landsat thematic mapper thermal band. *Remote Sens Environ.*, 1989, 28, 339-47.
 2. Salisbury, J.W.; D'Aria, D.M. & Wald, A. Measurements of thermal infrared spectral reflectance of frost, snow and ice. *J. Geophys. Res.*, 1994, 99(B12), 24235-24240.

Contributors

Mr Fily is teaching at University Joseph Fourier of Grenoble in the field of Physics and Geophysics. He is the In-Charge of the Remote Sensing Group at the Laboratoire de Glaciologie and Geophysique de l' Environment. His areas of research include: antarctic ice sheet (solar spectrum and microwave remote sensing).

Mr JP Dedieu is working as Research Scientist at the Laboratoire de la Montagne Alpine, Grenoble. His areas of research include: remote sensing in the Alps for hydrological applications with active remote sensing sensors.

Mr Durand is working as Research Scientist at the Centre d'Etudes de la Neige, a research institute of the French Meteorological Institute. His areas of research include: atmospheric modelling and avalanche forecasting.

Mr Sergent is working as Research Engineer at the Centre d'Etudes de la Neige at Grenoble. His areas of work include: measurements of snow reflectance and avalanche forecasting.